SLAC – PUB – 3935
April 1986
(A)

COMPARISON OF STANDING-WAVE AND TRAVELING-WAVE STRUCTURES*

ROGER H. MILLER
Stanford Linear Accelerator Center
Stanford University, Stanford, California 94305

Introduction

The controversy over the relative advantages of standing-wave and traveling-wave linear accelerators is now in its fourth decade. It has been fed by a considerable body of misinformation. The author hopes in this paper to shed some light on the subject, and expose some of the falsehoods. The discussion is directed toward the question of which structure to use for short pulse high field electron accelerators since it is almost universally accepted that standing-wave structures are appropriate for CW and long pulse accelerators. Three arguments against standing-wave accelerators are discussed and shown to be invalid.

The Stanford Myth

The Stanford myth states that a standing-wave can be considered to be the superposition of two traveling waves (true!). It further states each of these traveling waves contributes equally to the power dissipated in the structure (true!) but that only the wave traveling in the same direction as the particle contributes significantly to the acceleration (usually true?). Thus, concludes the myth, since the acceleration is equal to a single traveling wave but the power dissipated is twice as great, the shunt impedance of a standing wave accelerator is half as large as that for the traveling wave:

$$r_{SW} = \frac{1}{2} r_{TW} \qquad \text{Stanford Myth}$$

where

r_{SW} = shunt impedance of standing wave
r_{TW} = shunt impedance of traveling wave

In either case the shunt impedance is defined as

$$r \equiv \frac{E_{ave}^2}{dP/dZ}$$

where

E_{ave} = the average accelerating field seen by the particle
dP/dZ = power dissipated in the structure per unit length

The Stanford myth is mostly true and yet irrelevant and consequently false. It is irrelevant because it does not apply to the structures always used in SW accelerators for reasons we shall see.

In Fig. 1a, a coaxial line is shown with a TEM wave traveling from left to right. The coax line has three radial electric field probes spaced $\lambda/2$ apart through its upper wall, and four probes spaced $\lambda/3$ apart through its lower wall. Figure 1b shows the radial electric field E_r as a function of Z at time $t = 0$. As time progresses the sinusoidal field pattern in Fig. 1b will move from left to right. In Figs. 1c and d respectively, we show the signals on the $\lambda/2$ spaced probes A, B, C and the $\lambda/3$ probes D, E, F, G as a function of time. It is apparent from Fig. 1c that it is impossible to determine from the $\lambda/2$ electric field probes whether the wave is traveling from left to right, i.e., from A to B to C or from right to left, i.e., from C to B to A. It follows that two equal waves traveling from opposite directions (i.e., a standing wave) could also give the the signals seen on probes A, B. and C. Conversely, it is apparent from the signals from the $\lambda/3$ probes in Fig. 1d that the wave is traveling from D to E to F to G, i.e., from left to right. A more careful consideration of Fig. 1d suggests a second possibility: the wave could be traveling from right to at half the velocity since it takes twice as long as seen by the probes for the wave to go from E to D as it does to go from D to E.

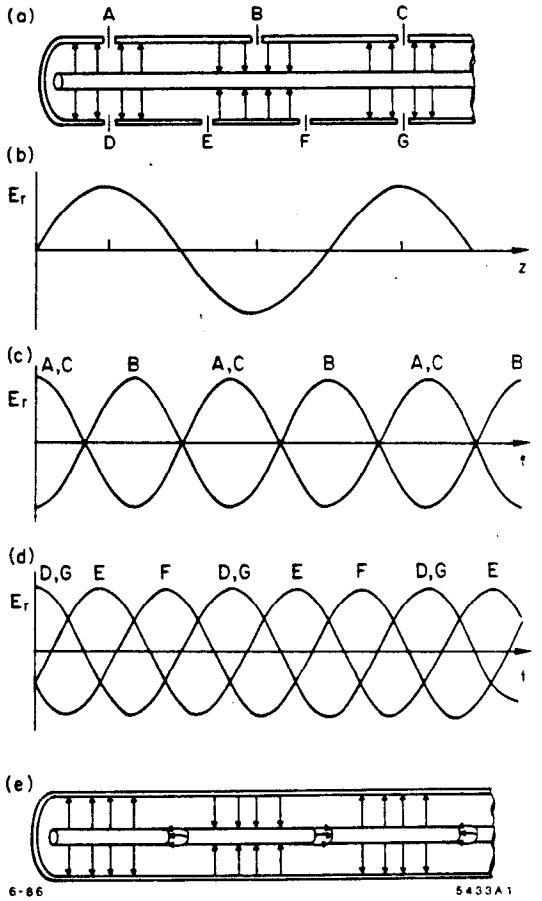

Fig. 1. Electric fields in a coaxial line: a) The coaxial line; b) Radial electric field as a function of distance along the line; c) Radial electric field at $\lambda/2$-spaced probes vs. time; d) Radial electric field at $\lambda/3$-spaced probes vs. time; e) A hypothetical π-mode linac made from the coaxial line.

The coaxial line in 1a can, in principal, be made into a particle accelerator by introducing gaps into the hollow center conductor as shown in Fig. 1e. Interrupting the current flow in the center conductor will produce longitudinal electric field across the gaps which will accelerate charged particles traveling inside the center conductor. If the gaps are placed every half-wavelength, it follows from our discussion above, the particles will be accelerated whether they are going the same direction or the opposite as the wave. Therefore, both traveling-wave components contribute equally to the acceleration of the particles. Thus the conclusion of the Stanford Myth does not apply. If, instead, we had spaced the gaps at intervals of $\lambda/3$ we

*Work supported by the Department of Energy, contract DE-AC03-76SF00515.

Invited paper presented at the Stanford Linear Accelerator Conference, Stanford, California, June 2-6, 1986

would find we could accelerate particles moving only in the same direction as the wave if their velocity was equal to the phase velocity of the wave. Particles moving half as fast could be accelerated in the opposite direction.

We gain additional insight if we consider the standing-wave accelerator to be a chain of N coupled resonators. The voltage across the accelerating gap of the n^{th} resonator is:

$$V_n = V_0 \cos\frac{(n-1)\pi q}{N-1}\cos wt \tag{1}$$

where $\pi q/(N-1)$ is the phase shift from cell to cell in a traveling wave. The resonance condition requires that q be an integer such that

$$0 \le q \le (N-1)$$

The time when a particle gets to the center of the n^{th} gap is

$$t = \frac{Z}{v} = (n-1)\frac{\ell}{v}$$

where

v is the particle velocity
ℓ is the periodic length

$$V_n = V_0 \cos\frac{(n-1)\pi q}{N-1}\cos w\frac{(n-1)\ell}{v} \tag{2}$$

Maximum energy gain occurs for the synchronism condition

$$\frac{w\ell}{v} = \pi\left(\frac{q}{N-1} + 2p\right)$$

where p is an integer.

Then the total voltage gain is

$$V = \sum_{n=1}^{N} V_n = V_0 \sum_{n=1}^{N} \cos^2\frac{(n-1)\pi q}{N-1} \tag{3}$$

$$V = \frac{NV_0}{2} \quad \text{for} \quad 0 \neq q \neq N-1 \tag{4}$$

When

$$\begin{aligned} &q = 0 \quad \text{or} \quad N-1 \\ &V = NV_0 \end{aligned} \tag{5}$$

Note that the factor $1/2$ for other than 0 or π modes arises from two factors: 1) the voltages across the gaps are not all equal but rather have a cosine distribution,

$$\cos\left[\frac{\pi(n-1)q}{(N-1)}\right]$$

and 2) the particles don't arrive at the gaps at the maximum field time but rather there is a cosine phase dependence,

$$\cos w\frac{(n-1)\ell}{v} \quad .$$

We are now ready to calculate the shunt impedance. When

$$0 \neq q \neq (N-1)$$

the power dissipated is

$$\begin{aligned} P &= \frac{1}{R_c}\sum_{n=1}^{N} V_n^2 \\ &= \frac{NV_0^2}{R_c}\sum_{n=1}^{N}\cos^2\frac{(n-1)\pi q}{N-1} \end{aligned}$$

where R_c is the single cell shunt impedance.

$$P = \frac{N}{2R_c}V_0^2$$

The total structure shunt impedance is

$$R_T \equiv \frac{V^2}{P} = \frac{\left(\frac{NV_0}{2}\right)^2}{\left(\frac{N}{2R_c}V_0^2\right)}$$

$$R_T = \frac{N}{2}R_c \qquad 0 \neq q \neq N-1 \tag{6}$$

For $\pi q/(N-1) = 0$ or π or for traveling wave

$$P = \frac{NV_0^2}{R_c}$$

$$V = NV_0$$

$$R_T = NR_c\,; \qquad \frac{\pi q}{N-1} = n\pi \tag{7}$$

Needless to say almost all standing-wave accelerators are built in 0 mode or π mode (i.e., $\pi q/(N-1) = 0$, or π). However, until the early sixties these modes had one very serious drawback, the group velocity is approximately zero. The group velocity is the energy propagation velocity. A zero group velocity means the structure is poor at delivering energy to the beam and that the field profile is very sensitive to beam current and mechanical tolerance. The development in the early sixties of what is sometimes called resonant coupling eliminated this problem. The resonant coupling as developed at Los Alamos[1] for π mode structures is best understood by considering the case for $q = 4$ in Eq. (1), i.e., $\pi q/(N-1) = \pi/2$. In fact, it is a semantic question whether the Los Alamos structure is $\pi/2$ mode or π mode. For $q = 4$ Eq. (1) becomes

$$V_n = V_0 \cos(n-1)\frac{\pi}{2}\cos wt \tag{8}$$

when we see that $V_n = V_0$ when n is odd and $V_n = 0$ when n is even. The shunt impedance is

$$R_T = \frac{N}{2}R_c$$

but that is not surprising since half the cells have zero fields. Since the voltage across the even numbered cells is zero, there is no need for them to be on the beam axis, so Los Alamos moved them off-axis and created the side-coupled structure shown in Fig. 2. This structure is electrically a $\pi/2$ mode, but in terms of its interaction with beams it is a π-mode structure. An alternative to moving the unexcited or coupling cavities off-axis is to shrink their length as shown in the "on-axis" coupled structure also shown in Fig. 2. Since these structures are electrically a $\pi/2$ mode, they are in the middle of the pass band (half-way between 0 mode and π mode) where the group velocity is the greatest.

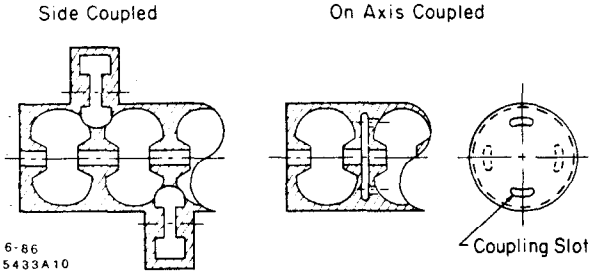

Fig. 2. Two biperiodic (resonantly coupled π-mode) linac structures.

One may ask how close to π mode must one be for $V = NV_0$? The answer is that if the structure is exactly periodic and the boundary condition $\pi q/(N-1) = m\pi$ with m an integer is met exactly, then the structure must be exactly π mode. For example, if the phase shift per cell is exactly $99\pi/100$ the structure must be 100 cells long to meet the periodic boundary condition and one finds $V = (N/2)V_0 = 50V_0$.

Reality, of course, is never perfect and no structure is perfectly tuned. If the terminations have an appropriate reactance a 30 cell structure could be resonant in the $99\pi/100$ mode. If the resonant frequency of the first and last cavity is the same and adjusted appropriately, the maximum field can be in the center of the structure. In this case one gets a shunt impedance which is 93% of the π-mode shunt impedance or in other words a shunt impedance per cavity which is 93% of the single-cavity shunt impedance.

Z. D. Farkas[2] calculated the shunt impedance per unit length for a disk-loaded waveguide structure shown in Fig. 3.

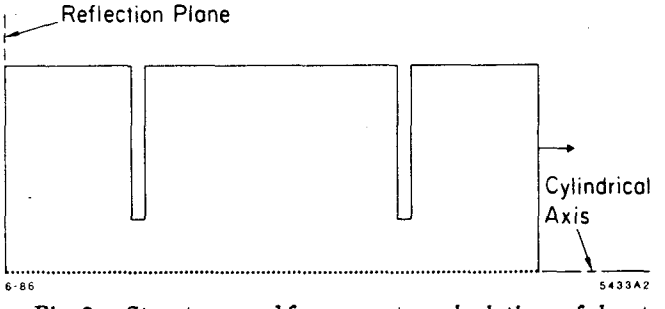

Fig. 3. Structure used for computer calculations of shunt impedance in Fig. 4.

He calculated the shunt impedance for a number of traveling wave modes using the program KN7C.[3] He then calculated the shunt impedance for the same modes as standing waves in the same structures using the program URMEL.[4] Finally, he made a series of calculations of standing-wave structures in which the end cells were not standard. This was done by moving the right-hand boundary in Fig. 3 so the right-hand cell was not precisely half of the other cells. Since the left-hand boundary is a Neumann boundary, the structure being calculated is a structure with symmetry around the left boundary. That is, a structure with three full equal cells and with identical partial cells on each end. By moving the right-hand boundary he was able, in effect, to tune the resonant frequency of the end cells in a five-cell structure. The shunt impedances calculated are shown in Fig. 4.

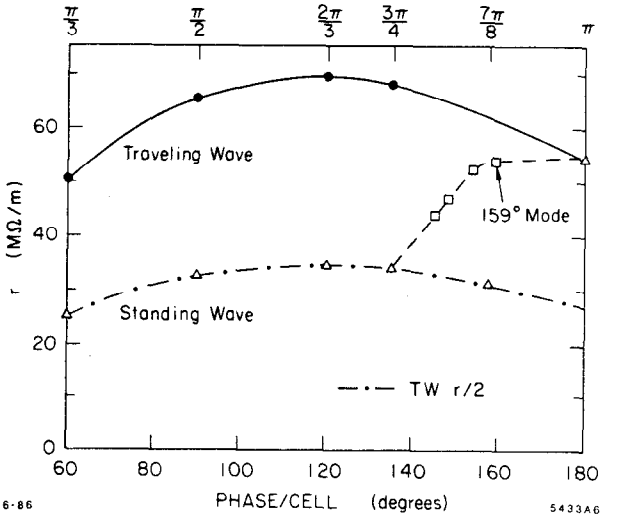

Fig. 4. Shunt impedance of traveling- and standing-wave modes in disk-loaded waveguide.[2]

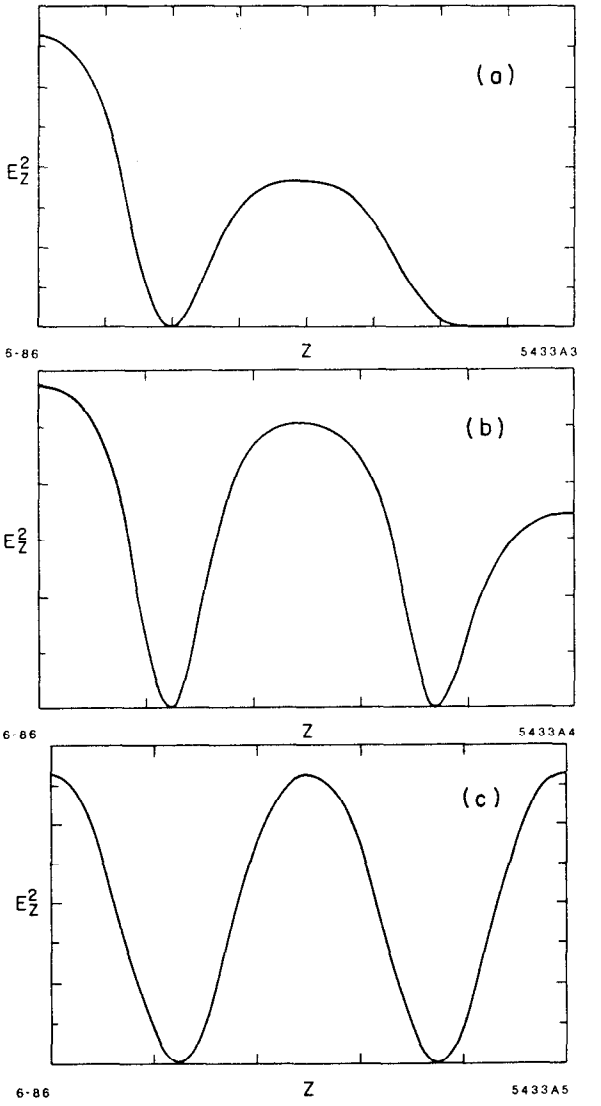

Fig. 5. Field distributions for three standing-wave modes shown in Fig. 4: a) $3\pi/4$-mode; b) 159°-mode; c) π-mode.

The standing-wave modes with the periodic boundary condition of Eq. (2) are shown as triangles. They have half the shunt impedance per unit length of the same mode in a traveling wave with the exception of the π mode. The standing-wave modes with aperiodic boundary conditions are shown as squares. They lie on a continuous curve between the $3\pi/4$ mode on the $V_{TW}/2$ curve to the π-mode on the V_{TW} curve. This transition can be understood by considering Fig. 5a, b and c, in which $E_z^2(z)$ is plotted for the $3\pi/4$ mode, the 159°-mode and the π-mode respectively. It is apparent that the field strength gets progressively more uniform from cell to cell as one moves from the $3\pi/4$-mode with periodic boundaries to the 159°-mode with aperiodic boundaries to the π-mode.

Reflections from Standing-Wave Accelerators

Reflections from standing-wave accelerators are a serious concern because klystrons can be destroyed by reflected power. Any high q resonant cavity reflects a large fraction of the incident power during the beginning of the filling time. Furthermore, a standing-wave accelerator can only be matched for some nominal current. For either a higher or lower current, power will be reflected from the structure. For low-power accelerators the solution is normally to put an isolator or a circulator between the klystron or other microwave source and the load. However, isolators do not presently exist for the very high power levels used in most high energy short pulse linear accelerators. Fortunately, a very simple remedy exists. If each klystron drives two standing wave accelerator sections (Fig. 6) through a 3 db hybrid, if the waveguides to the sections are equal in length, and if the two sections present the same impedance to the waveguide, then the reflections will add constructively in the fourth arm of the hybrid.

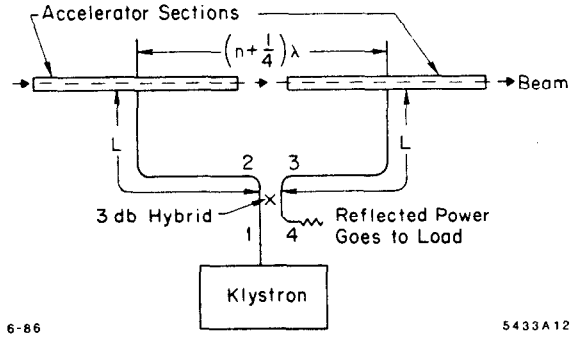

Fig. 6. Configuration for avoiding reflection from standing-wave structure.

Thus the reflected power will go to the dummy load. This technique has been tested thoroughly at SLAC, for it is precisely the way the energy storage cavities in the SLED system work. Each SLAC klystron drives two SLED cavities (loaded $Q \approx 20{,}000$) through a 3 db hybrid and the reflected and reradiated power is transmitted through the fourth arm of the hybrid. In the SLED case the fourth arm goes to the accelerator rather than a dummy load. The reflected power from the SLED cavities would surely damage the klystrons were it not for the isolating property of the hybrid when used in this fashion. The 3 db hybrid gives only 6 db isolation against reflection from arcs in the structures, since the two structures will only very rarely arc in exactly the same place on the same pulse so as to produce the desired interference between the two reflected waves.

Filling Time for Standing-Wave Accelerators

Since any resonant system approaches steady-state exponentially, it takes quite a number of time constants to get very close to the steady state. For example, it takes 4.6 time constants to reach 99% of steady state; 6.9 time constants for 99.9%. However, for a modern high current, high energy accelerator designed for high energy and nuclear physics it is reasonable to design the structure so that the beam loaded energy is about 80% of the unloaded energy. A standing-wave accelerator reaches 80% of steady state in 1.6 time constants. The appropriate time constant is the time constant when loaded by input coupling iris:

$$\tau = \frac{2Q_0}{w(1+\beta)}$$

where β is the coupling constant which is measured as the VSWR with the beam off. Since the coupling is chosen so that the structure is approximately matched with beam on, this time constant may be a factor of three shorter than the unloaded time constant. In a study done by the author on a conventional standing-wave structure for CEBAF the time from the beginning of the RF pulse until the beginning of the beam pulse was .8 μsec (exactly the same as for the SLAC structure). However, the response of the standing-wave structure to an external RF pulse, and the response of the structure to a beam, are both exponentials with exactly the same time constant. Therefore, if the beam is turned on at precisely the instant when the structure reaches the steady-state value with the beam on, then the beam energy stays right at that steady state value as shown in Fig. 7.

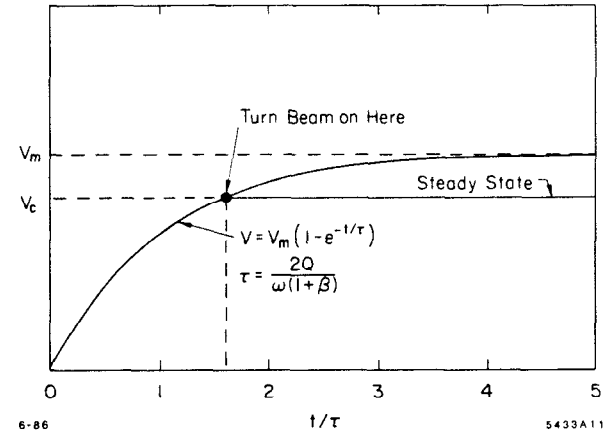

Fig. 7. Energy transients in standing-wave accelerators.

If less than full beam current is desired, the same procedure is followed except that when the beam is turned on, the RF power is reduced. The reduction of RF power can be accomplished by reducing the RF drive to klystrons with fast solid-state attenuators, or by removing the drive from certain klystrons with fast RF switches or a combination of both. The voltage through a standing-wave structure of length L is given by

$$V = (rLP)^{1/2}\left(\frac{2\beta^{1/2}}{1+\beta}\right)\left(1-e^{-t/\tau}\right) - \frac{irL}{1+\beta}\left[1-\exp\left(-\frac{t-t_b}{\tau}\right)\right]$$

where t_b is the time where the beam is turned on and the current $i = 0$ for $t < t_b$, and is constant for $t \geq t_b$. If one

chooses t_b so that

$$\frac{irL}{1+\beta} = (rLP)^{1/2}\frac{2\beta^{1/2}}{1+\beta}\exp\left(-\frac{t_b}{\tau}\right)$$

one finds that for $t \geq t_b$

$$V = (rLP)^{1/2}\left(\frac{2\beta^{1/2}}{1+\beta}\right)\left[1-\exp\left(-\frac{t_b}{\tau}\right)\right] \quad ,$$

so V is constant for $t \geq t_b$. It follows that the right time to turn the beam on is

$$t_b = \tau\ell n\frac{irL}{2\beta^{1/2}(rLP)^{1/2}}$$

If β has been adjusted so that there is no reflection from the structure when the beam is on, this can be expressed as

$$t_b = \tau\ell n\frac{\beta-1}{2\beta} \quad .$$

This procedure for compensating for the beam loading energy transient is easier than that employed in traveling-wave accelerators. With traveling-wave accelerators, the response of the structure to the beam has a different functional dependence on time than the response to an external RF source. Hence, to get good beam loading compensation, it is necessary to turn on the compensating klystrons at a number of different times in order to synthesize the inverse of the beam loading transient with the klystrons.

Quantitative Comparison

Now that we have discussed the three major considerations that were once thought to eliminate standing-wave structures as candidates for short pulse, high energy electron linacs, we must look quantitatively at both standing-wave structures and traveling-wavestructures to see which is superior. From Fig. 4, we might conclude that the $2\pi/3$ traveling wave strcture was the clear choice since it has the highest shunt impedance, about 20% higher than the π-mode. The reason for this is that the calculations were done for the flat disk-loaded waveguide shown in Fig. 3. The shunt impedance per unit length falls off to the left of $2\pi/3$ because the increasing number of disks per unit length increase the conductor surface areas per unit length and hence the losses. To the right of $2\pi/3$ the shunt impedance decreases because the transit time factor

$$T \approx \frac{\sin\Delta\phi/2}{\Delta\phi/2}$$

decreases rapidly beyond a phase shift per cell $\Delta\phi$ of 120°. However, nose cones or drift tubes can be added to the disks so that the accelerating gap need not increase in length as the number of cells per wavelength decreases. In this case the shunt impedance increases monotonically with increasing phase shift up to π mode.

The side coupled structure shown in Fig. 2 has been optimized in recent years to achieve shunt impedances in excess of 100 MΩ/m at S-band as compared with 57 MΩ/m for the SLAC strcture. The very high shunt impedances are obtained by reducing the beams aperture to 6 mm diameter—smaller than most accelerator designers would feel comfortable with for a long research accelerator. However, a shunt impedance of 80 MΩ/m can be obtained at 2856 MHz with a 10 mm diameter beam aperture. This cavity is scaled (and slightly modified) from the structure designed by LANL, for the NBS Microtron.[5,6] The nose cone shape, cavity radius, and gap length are optimized for shunt impedance.

Similar optimization can be done for traveling wave structures. Three possible designs are shown in Fig. 8. Figure 8a is a standard $2\pi/3$ SLAC structure. The figure shows 1-1/2 cells from LALA computer output. Figure 8b is a modified structure with about 15% higher shunt impedance. Figure 8c is a $7\pi/8$ half-cell with the same shape as the optimized structure used in the NBS Microtron. The shunt impedance should be 78 MΩ/m. Magnetic field coupling holes would be required between cells since coupling through the beam hole would be extremely small. This cavity has not been physically modeled. At the $7\pi/8$ mode, v_g is only 38% of the midband value, so the coupling slots will need to be large and the coupling losses might be excessive. The optimum may be somewhere between $3\pi/4$ and $7\pi/8$.

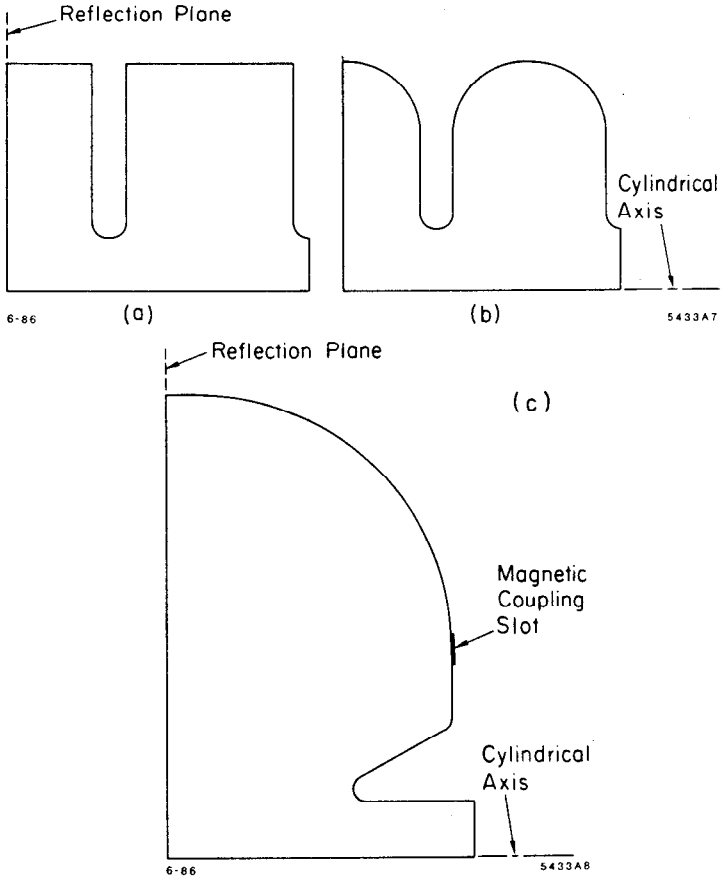

Fig. 8. Traveling-wave structures: a) SLAC $2\pi/3$ disk-loaded structure, r = 57 MΩ/m; b) SLAC $2\pi/3$ modified to raise Q, r = 65 MΩ/m; c) Optimized $7\pi/8$ travelling-wave structure, $r \approx$ 78 MΩ/m.

The author participated in a design study carried out at CEBAF which attempted to compare these structures with side coupled standing-wave structures. For a constant gradient traveling-wave structure the power required to achieve a

voltage gain of V in an accelerator structure is

$$P_{TW} = \frac{1}{r\ell(1-e^{-2\tau})}\left[V + \frac{ir\ell}{2}\left(1 - \frac{2\tau e^{-2\tau}}{1-e^{-2\tau}}\right)\right]^2$$

where τ is the attenuation through the structure.

For the standing-wave structure

$$P_{SW} = \frac{(1+\beta)^2}{4r\ell\beta}\left[V + \frac{ir\ell}{(1+\beta)}\right]^2$$

For each of the traveling-wave structures except the SLAC structure, the attenuation was chosen to minimize the average power required. For the SLAC structure the attenuation was .57, i.e., the actual value for the existing SLAC structure. The following parameters were fixed by other aspects of the CEBAF design:

Linac energy	= 2 GeV
Linac active length	= 105 meters
Peak current	= 200 mA
Beam pulse length	= 2.4 μsec

A comparison of the different structures is shown in Table 1.

Table 1

Structure	r (MΩ/m)	r_{eff} (MΩ/m)	β	τ	$\frac{r_{eff}}{r_{scs}}$	Linac Cost $M
Side coupled (SCS)	80	80	2		100%	30
Optimized $7\pi/8$ TW (Fig. 8c)	78	67		.7	84%	33
Modified SLAC (Fig. 8b)	66	56		.65	70%	34
SLAC (Fig. 8a)	57	44		.57	55%	35

The effective shunt impedance r_{eff} includes the power lost in the load for the traveling-wave or reflected in the standing-wave structure. For the side-coupled structure in this example, this turned out to be negligible at full current when the average power had been minimized. For the traveling-wave structure the load power varied from about 20% to 15%. The choice probably finally comes down to economics and so the last column gives estimated costs for the linacs including klystrons, klystron modulator, rectangular waveguide, and accelerator structure, but no instrumentation and control, no beam steering and focusing. The SLAC structure was estimated to cost about 20% less per unit length than the side-coupled structure, but required 80% more RF power and hence the increased cost of klystrons and modulators made the overall cost of the accelerator more expensive. The author is happy to let each reader do his own cost estimates.

A comparison was also done for a CEBAF design in which the beam was not recirculated through the linac. For this case the overall length of the accelerator became a free parameter to be optimized and the beam pulse length was 1.2 μsec. This case also favored the standing-wave structure by about 10% in costs.

Standing-wave accelerator structures are certainly competitive and probably superior in the domain of short pulse electron linacs, which for many years have been considered to be the exclusive domain of traveling-wave structures. The one parameter region in which traveling-wave structures are probably superior is when the beam pulse is negligibly small compred with the natural time constant of the structure, $\tau = 2Q/\omega$, such as linear colliders and storage ring injectors. This is particularly true when energy storage cavities are used for pulse compression (e.g., SLED). The RF pulse from such systems has the form

$$P_{(t)} = P_0\left(1 - e^{-t/\tau}\right)$$

so the power incident on the structure is maximum when the reflection coefficient from a standing-wave structure is maximum.

Acknowledgement

The author wishes to thank the staff at CEBAF where much of the work leading to this paper was done for their hospitality and support, Bill Diamond, Richard York, Stan Schriber, Dave Farkas and Greg Loew for helpful discussions, Masry Menzel of Los Alamos for shunt impedance calculations, and Bette-Jane Ferandin and the SLAC Technical Illustrations Group for their patient assistance in preparing this paper.

References

1. D. Nagle, E. A. Knapp and B. C. Knapp, Rev. Sci. Instrum. **38**, 1583 (1967); E. A. Knapp, B. C. Knapp and J. M. Potter, Rev. Sci. Instrum. **39**, 979 (1968).
2. Z. D. Farkas, Unified Formulation for Accelerator Design, SLAC-PUB-3981, May 1986.
3. E. Keil, N.I.M. **100**, 419 (1972).
4. T. Weiland, N.I.M. **216**, pp 329-348 (1983).
5. Radio-Frequency Structure Development for the Los Alamos/NBS Racetrack Microtron, compiled and edited by R. A. Jameson, R. H. Stokes, J. E. Stovall, and L. S. Taylor, LA-UR-83-95.
6. Accelerator Technology Program, Jan-Sept 1983, LA-10191-SR, compiled by R. A. Jameson, p. 23-29.